Stabilization of cholesteric blue phases using polymerized nanoparticles

Emine Kemiklioglu,* Jeoung-Yeon Hwang, and Liang-Chy Chien
Liquid Crystal Institute and Chemical Physics Interdisciplinary Program, Kent State University, Kent, Ohio 44242, USA
(Received 23 August 2013; published 16 April 2014; corrected 5 June 2014)

This study explores the roles of UV-polymerizable silicon-based nanoparticles in polymer-stabilized blue phase (PSBP) liquid crystals. Our analysis reveals that the polymerized polymer leads to widening of the temperature range of the blue phase and stabilization of the reflection wavelength against temperature variations. A polymer morphology study of PSBP reveals the polydomain nature of the blue phase. In practical application, the advantage of the low-surface-energy property of the UV-polymerizable silicon-based nanoparticles leads to a significant reduction in switching voltage from 140 to 40 V.

DOI: 10.1103/PhysRevE.89.042502 PACS number(s): 61.30.−v

I. INTRODUCTION

Blue phases (BPs) are structures in which the molecules are organizing themselves into complex three-dimensional (3D) structures characterized by crystallographic space-group symmetry. Hence, blue phases form as double-twisted cylinders separated by defect lines. Effectively, it is the network of the defect lines that characterizes the blue phases. Three network states are known to form with increasing temperature: These are denoted as BPI, BPII, and BPIII. The BPI and BPII states form soft, frequently coagulating platelet domains with sizes in the range of micrometers to submillimeters. The Bravais lattice is body centered for BPI and simple cubic for BPII [1]. Indeed, light is selectively reflected from BPs, with the scattering vectors forming a reciprocal lattice of a cubic periodic system. The lattice constant is a few hundred nanometers depending on the radius of the double-twisted helix, and the photonic band, which is mostly in the blue wavelength range, is of the same order of magnitude as the cholesteric pitch. BPIII has a cloudy and amorphous appearance and is called "blue fog."

Previously, blue phases were a challenge to researchers because they require extreme temperature stabilization. Thermodynamically stable blue phases having low-chirality chiral nematic behavior were predicted using the Landau theory [2], and it was demonstrated that the planar helix structure that is generally associated with the cholesteric phase becomes unstable at a temperature near the transition point. Further, as explained by Meiboom *et al.* [3] on the basis of the Oseen-Frank elasticity equation, as an alternative, the temperature range of the blue phase liquid crystal (BPLC) can be estimated according to Meiboom's defect model. However, the surface energy at the interface between the core and cholesteric BP was "simplified" and assumed as being zero during energy minimization for the system.

The Skyrmion arrangement requires a high bend curvature of the director to stabilize the blue phase. Recently, Castles *et al.* [4] used a mixture of nematic bimesogenic liquid crystals to stabilize the defect structures against temperature variation and obtained blue phases over a range of about 50 °C. This stabilization, which resulted from the flexoelectric coupling between the polar order and the curvature of the director, was considered to be the reason for the change in properties of the blue phase [5,6]. Alternatively, Kikuchi *et al.* [7–9] developed a technique for broadening the blue phase temperature range by using a polymerized polymer network, referred to as the polymer-stabilized blue phase (PSBP). Through synchrotron small angle x-ray scattering measurement, the polymers in the PSBP were found to form a remarkably unique aggregation structure, which was selectively concentrated in the disclination cores [10]. This result clearly corroborates the mechanism of the stabilizing effect of BPI resulting from the immobilization of the disclination cores in the blue phase by polymers and would enable the development of high-performance Kerr devices. Similarly, an electrical-field-switched color filter using a PSBP liquid crystal in which the Bragg-reflected color of the blue phase can be switched to reflect colors can be used. The phase-separated 3D polymer network transcribes the cubic structure of a BPLC and restrains the deformation of the cubic lattice by the external electric field. These wide-range electric-field-switched color filters with PSBP may be an important step toward the development of ecofriendly color reflective displays [11]. Polymer-modified carbon nanotubes [12,13] and nanoparticles [14–18] have attracted considerable research attention and interest because of their potential to exhibit dramatically enhanced mechanical, electrical, and thermal properties.

This paper presents an investigation of an organic-inorganic composite that may ultimately enable us to achieve the above-described objectives of broadening the temperature range of blue phases and developing a high-performance Kerr device [19]. Our goal is to predicatively understand how organic-inorganic nanocomposites can be used to stabilize the blue phase, develop and characterize these nanocomposites, and systematically modify the surface energy at the interface between the core and the cholesteric liquid crystal, which was previously simplified. To address this issue, we use a mixture of monomers consisting of a monomeric nanoparticle with an acrylate-polymerizable group, polyhedral oligomeric silsesquioxane [PSS-(1-propylmethacrylate)-heptaisobutyl (PSS-PMH, Aldrich Chemical)], and a commercially available mesogenic diacrylate RM257 (Merck). The molecules of polyhedral oligomeric silsesquioxane have nonreactive or reactive substituents at the corner silicon atoms. Because of the presence of the polymerizable organic methyacrylate, PSS-PMH molecules are compatible with both polymers and monomers. Addition of PSS-PMH

*ekemikli@kent.edu

derivatives to the polymeric systems may induce significant improvements in the polymer properties, such as a broadening of their use temperature, mechanical properties, and their viscosity [20–22]. Unlike many other nanoparticles, PSS-PMH nanoparticles—which are expected to have low surface tension—can disperse easily in a wide range of polymer matrices. We expect the polymerized nanoparticles to accumulate in the defect cores owing to the size of these nanoparticles, which will lower the interfacial energy. Furthermore, the nanoparticles are expected to disrupt any tendency toward orientational order inside the core as temperatures decrease into the blue phase. However, most of the research has focused on expanding the BP temperature range as well as improving the electro-optical properties by doping nanoparticles [23,24]. Here we used a monomeric nanoparticle with an acrylate-polymerizable group. The inorganic PSS-PMH segments covalently bind to the polymer network and thus provide unique opportunities for stabilizing the blue phases, on account of the size and van der Waals interactions of the polyhedral oligomeric silsesquioxane functional groups with cholesteric BP liquid crystals.

II. EXPERIMENT

A representative BPLC material comprising 55 wt % of a commercially available nematic liquid crystal [BL006 and MLC6080 (Merck)] and 45 wt % of a chiral dopant (20% CB15, 20% R811, and 5% R1011) was used. A mesogenic diacrylate monomer (bis[acryloyloxy-(4-propoxyl-(1,4-phenybenzoate))]) RM257 (Merck), PSS-PMH monomer, and a small amount of photoinitiator (0.01 wt % of Irgacure 651 by weight of a reactive monomer and BPLC mixture) were added to the BPLC mixture. The transition temperature and reflection spectra were measured using planar glass cells separated by glass ball spacers to give a cell gap of 15 μm. All samples were heated to the isotropic phase and cooled to room temperature at a rate of $-0.2\,^{\circ}\mathrm{C/min}$. The optical textures were observed with a polarizing optical microscope (POM), and the samples were placed on a hot stage equipped with a programmable temperature controller and positioned between a pair of polarizers crossed at 90°. Reflection spectra were measured with an Ocean Optics spectrometer at various temperatures.

In-plane-switching (IPS) cells were prepared with an interdigitated indium tin oxide (ITO) electrode that was lithographically patterned to give an electrode width of 10 μm and electrode space of 10 μm on one glass substrate. The IPS cells were assembled by placing a second substrate without an ITO electrode on top of the first substrate, and the two substrates were separated by 10-μm glass ball spacers to give a cell gap of 10 μm (this cell configuration is referred to as 10/10/5).

The mixtures of the reactive monomer and BPLC were filled into the cells, and the cells were exposed to a UV lamp (365 nm, 0.4 $\mathrm{mW/cm^2}$) from the electrode side for 40 min at the BPII temperature of the blue phase mixtures before polymerization. An in-house assembled electro-optic (EO) apparatus consisting of a helium-neon laser with light emission at 633 nm, a pair of polarizers crossed at 90° with respect to the polarization axes, a diode detector, a computer-controlled function generator, and an amplifier was used for data acquisition. The plots of light transmittance as functions of applied voltage and response times were acquired at blue phase temperatures.

A morphological study of the samples was conducted by extracting BPLC from the cell using a mixture of dichloromethane and hexane in a ratio of 20:80. The cell was opened and dried under reduced pressure. The polymer was sputtered with a thin layer of gold and examined with a Hitachi S-2600N scanning electronic microscope (SEM).

III. RESULTS AND DISCUSSION

In order to investigate the effects of the polymer network on the blue phase behavior, samples with different monomer concentrations were formulated; the compositions of these samples are listed in Table I. Samples 1, 2, and 3 contain the nematic liquid crystal BL006, whereas sample 4 consists of a mixture of nematic liquid crystals BL006 and MLC6080 in a 1:1 ratio mixed at the same ratio of nematic to chiral dopant. The pure blue phase mixtures of samples 1, 2, and 3 showed isotropic-to-blue-phase transition at 41.8 °C and blue-phase-to-cholesteric-phase transition at 32 °C. The blue phase was observed over a wider temperature range in the case of using the mixture of MLC6080 and BL006 (sample 4). This sample showed the isotropic-to-blue-phase transition at 43.8 °C and the blue-phase-to-cholesteric-phase transition at 30.7 °C. The bend-to-splay elastic constant ratio (K_{33}/K_{11}) of nematic BL006 is 1.86. The average bend-to-splay elastic constant ratio (K_{33}/K_{11}) of sample 4 is $[(1.32 + 1.86)/2] = 1.59$. These results suggest that the blue phase temperature range is associated with the value of the K_{33}/K_{11} ratios [25]. A decrease in the K_{33}/K_{11} ratio causes a broadening of the blue phase temperature range (see Supplemental Material [26]).

Blue phase textures of all PSBP samples were initially observed to have small colored domains, and the domain size was found to increase with a decrease in temperature

TABLE I. Compositions of monomer mixtures of RM257 and PSS-PMH and transition temperatures of PSBPs.

Sample	Monomer conc. (wt%) (RM/PSS-PMH)	BP temp. range before polymerization (°C)	(ΔT) (°C)	BP temp. range after polymerization (°C)	(ΔT) (°C)
1	6 (1:2)	57–39	18	59–40.8	18.2
2	8 (1:1)	53–42.2	10.8	52–39.5	12.5
3	10 (1:4)	51.8–40.5	11.3	55–40.5	14.5
3*	10 (10:0)	49.7–41	8.7	55.5–41.5	14
4	10 (1:4)	44.3–33	11.3	45.4–15	30.4

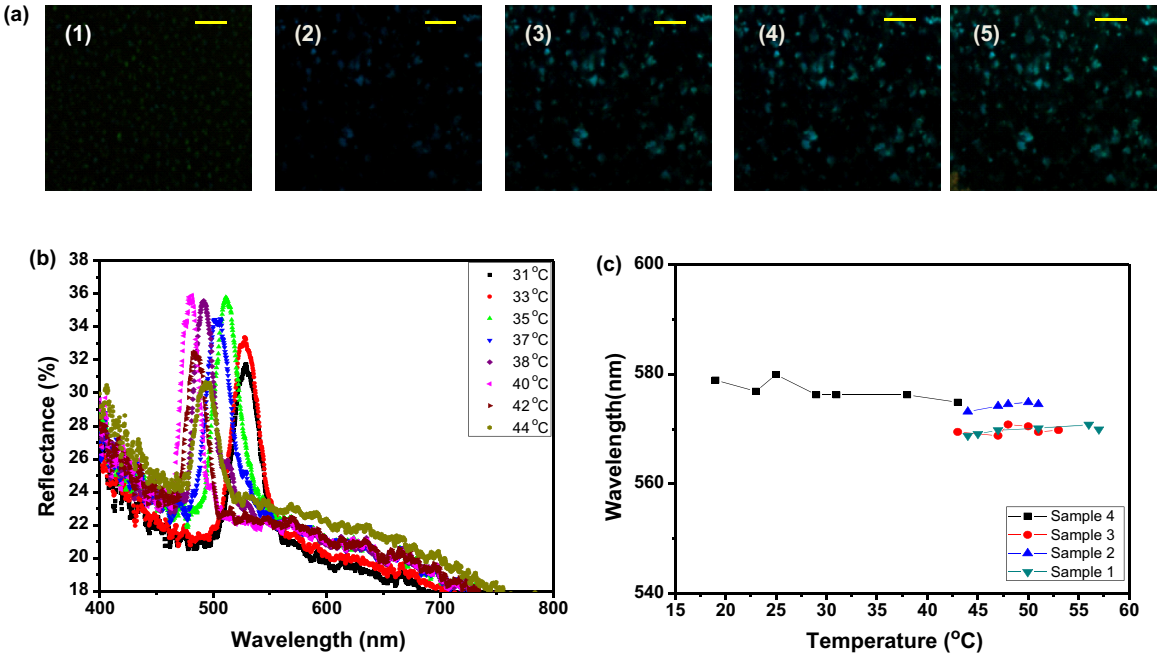

FIG. 1. (Color online) (a) POM images of BP textures of sample 4 at (1) 44.5 °C, (2) 38 °C, (3) 23 °C, (4) 17 °C, and (5) 16 °C, after polymerization. The scale bar is 20 μm. (b) Reflection spectra of pure BPLC without monomer. (c) Plot of wavelength versus temperature for samples 1 (at 570 nm), 2 (at 574 nm), 3 (at 570 nm), and 4 (at 576 nm) after polymerization.

as a result of distortion of the cubic lattice. According to the POM observations, the blue phase temperature ranges were broader than the temperature ranges of the mixtures before polymerization. In order to evaluate the stabilization of the blue phase, PSS-PMH was replaced with RM257 with a concentration of 10% (sample 3* in Table I). This substitution of RM257 did not have any significant effect on the blue phase stabilization. PSS-PMH nanoparticles disperse easily in a wide region of the blue phase mixture owing to a branched structure of the side alkyl group in the polymer.

Figure 1(a) shows the POM images of the PSBP sample 4 at various temperatures after polymerization. As seen in Fig. 1(b), the reflected wavelength of pure BPLC is blueshifted or redshifted when the temperature is increasing or decreasing, respectively. Further, as seen in Fig. 1(c), for the PSBP sample, the reflected wavelength was pinned at the same wavelength when temperature was ascending or descending, accordingly. Evidently, the PSBP cell showed good thermal stability against temperature fluctuation, as a result of stabilization of the polymer network in the disclination lines.

Figure 2 shows the EO properties of the studied PSBP samples. The results indicate that the threshold voltage V_{10}, i.e., the voltage required for achieving 10% transmission of the cell, is sensitive to the polymer concentration. Upon application of a sufficiently high in-plane voltage through the cells, we are able to switch the cells from an initial dark (field-off) state to a bright (field-on) state. For the BPLC sample without a monomer, the threshold voltage is 14.16 V.

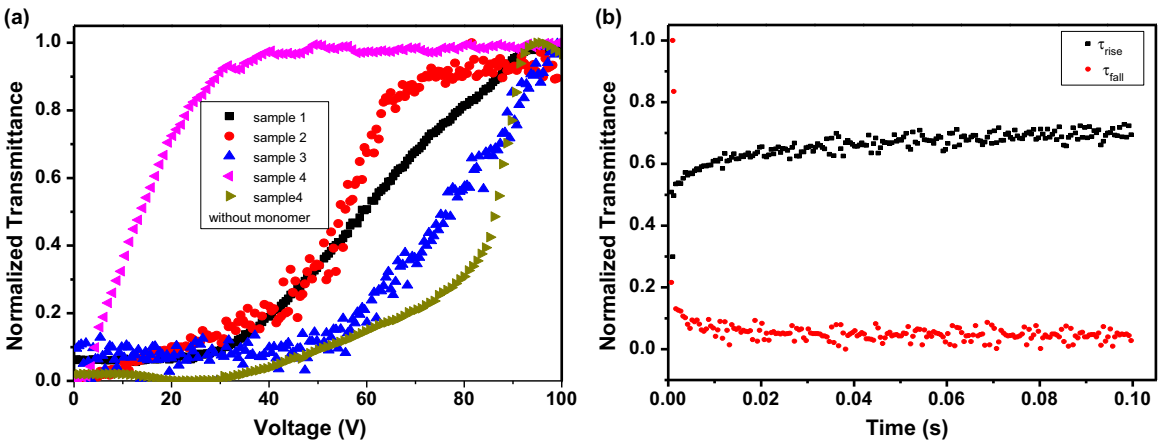

FIG. 2. (Color online) (a) Normalized transmittance-voltage (TV) curves of samples 1 (at 45 °C), 2 (at 45 °C), 3 (at 45 °C), 4 (at 35 °C), and sample containing mixture of BL006 and MCL6080 (at 40 °C without monomer). The BP temperature range increased to a higher temperature than that for the mixture before polymerization. (b) Plot of transmittance versus response time for sample 4.

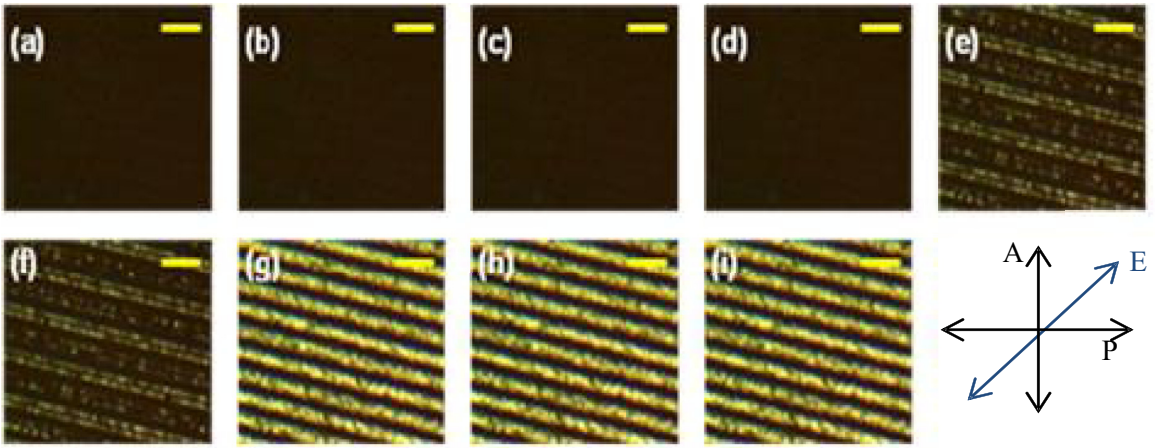

FIG. 3. (Color online) POM images of PSBP cell of sample 1 (6% polymer) under applied voltage of (a) 0 V, (b) 20 V, (c) 30 V, (d) 40 V, (e) 50 V, (f) 60 V, (g) 70 V, (h) 80 V, (i) 100 V with respect to the crossed polarizers labeled A and P at 45 °C. The black scale bar is 50 μm. A further increase in applied voltage causes a small shift in the spectral wavelength and increases light transmission for the samples.

Further, the threshold voltage for a BPLC sample is 36 V, whereas those for samples 1–4 are 29, 22, 11, and 4.5 V, respectively.

The turn-on voltages of these PSBP samples are also sensitive to the polymer concentration. For example, the turn-on voltages for samples 1–3 are 88, 78, and 89 V, respectively, at 45 °C. By contrast, the turn-on voltage for sample 4 is 30 V at 35 °C and that for a pure BPLC containing a mixture of two different nematic liquid crystals is 91.4 V at 40 °C. The switching voltage of sample 4 is lower than those of samples 1–3, the BPLC sample, and the reported PSBPs (which were switched at around 140 V) [5–9]. The low switching voltage of the reported PSBP samples is attributed to the polymerized nanoparticles, which disrupt any tendency toward orientational order inside the core of the blue phase and enable a weak anchoring at the surface of the inorganic nanoparticles. These results of low switching voltage distinguish this system from those of previously studied materials [27]. The advantages of the reported PSBP material are the temperature independence of the Bragg reflection and a low switching voltage.

Figures 3 and 4 show the POM images of samples 1 and 4, respectively, under an applied electric field. The deep color of the blue phase switches to a bright state at a low applied voltage. In the case of sample 1, the selective reflection of BPI switches from an initial deep blue color to a blue-green color at a voltage of 6 V μm^{-1} and 1 kHz. A further increase in applied voltage results in a small shift in the spectral wavelength and increases light transmission. The POM images show a few dark lines in the bright state, resulting from lithographically damaged electrodes. At applied voltages between 6 and 16 V μm^{-1}, the light transmission depends on the field strength. A further increase in the applied electric field results in a small spectral shift from blue to green, which is known as the extended Kerr effect in a PSBP composite [28]. The voltage-transmission curves of sample 4 shown in Fig. 2(a) validate this phenomenon. When the electric field is applied in the direction normal to the stripes, the cell starts to switch from an initial dark state at 40 V and achieves a bright state at 60 V.

The response times of the pure BPLC and PSBP samples are studied by switching between 10% and 90% light transmittance of the cells as obtained from Fig. 2(a). We determined the response times by switching sample 4 between its corresponding voltages V_{10} and V_{90} at 35 °C. The measured rise time (τ_{rise}) and fall time (τ_{fall}) for sample 4 are 6.2 and 4.5 ms, respectively. Further, τ_{rise} and τ_{fall} for sample 4 without a monomer are 1.1 and 0.7 ms, respectively.

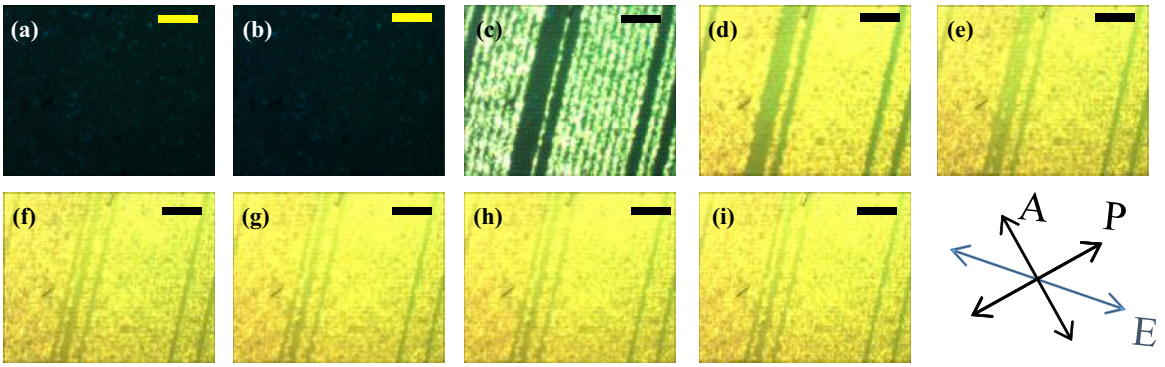

FIG. 4. (Color online) POM images of PSBP cell of sample 4 (10% polymer) under applied voltage of (a) 0 V, (b) 20 V, (c) 30 V, (d) 40 V, (e) 50 V, (f) 60 V, (g) 70 V, (h) 80 V, (i) 100 V with respect to the crossed polarizers labeled A and P at 35 °C. The black scale bar is 50 μm. A further increase in applied voltage causes a small shift in the spectral wavelength and increases light transmission for the samples.

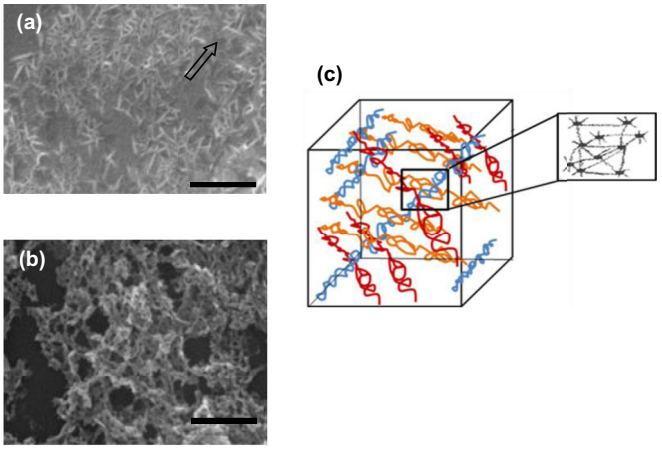

FIG. 5. (Color online) SEM micrographs of polymer morphology of PSBP cell of sample 4: (a) Surface of a substrate with electrode (the arrow indicates the electrode direction, which is the preferential orientation of polymer sticks), (b) surface of a substrate without electrode. The scale bars are 2 μm. (c) Simulated polymer network structure within a cubic lattice of a polymer-stabilized blue phase (the small cubes in the right-hand side image represent PSS-PMH).

The polymer network morphology was visualized using an SEM. The SEM image of the substrate with patterned electrodes viewed at a normal angle [Fig. 5(a)] reveals the formation of cubiclike patterns with submicrometer-sized polymer sticks having preferential orientation and aligned along the underlying interdigitated electrodes. This structure may be attributed to the grating effect of the UV light impinging on the reactive monomers. Therefore, the formation of polymer becomes anisotropic. These polymer sticks are between 300 and 600 nm in length, with a diameter of approximately 60 nm. By contrast, the SEM image of the polymer on the opposite substrate surface without electrodes shows connected hollow channels with a denser polymer intertwined in the bulk [Fig. 5(b)]. Because we placed a mirror behind the cell, the reflected light may have caused interference and destroyed the anisotropy of the light pattern. Therefore, the morphology was irregular. The size of empty tunnels ranged from a few hundred nanometers to 0.88 μm [29]. Figure 5(c) shows a simulated polymer network structure within a cubic lattice of a PSBP. The right-hand side image in Fig. 5(c) shows that PSS-PMH molecules are located at the joints of the polymer network; this is because the PSS-PMH monomer has a lower surface energy than that of RM257 and phase separates into the region of defects.

IV. CONCLUSION

We have demonstrated the stabilization of cholesteric blue phases using UV-polymerizable silicon-based nanoparticles to modify the interfacial properties of disclination cores and widen the temperature range of the blue phases. Our experimental results show that the concentration of PSS-PMH polymer plays an important role in the thermodynamic stability of modulated liquid-crystal blue phases. The low-surface-energy property of the inorganic PSS-PMH polymer leads to a significant reduction in the switching voltage of the corresponding device. It dramatically decreases the switching voltage from about 140 to 40 V. This significant reduction in the switching voltage and the widening of blue phase temperature range would be useful for new EO applications.

[1] P. Crooker, *Chirality in Liquid Crystals*, edited by H.-S. Kitzerow and C. Bahr (Springer, New York, 2001).
[2] D. C. Wright and N. D. Mermin, Rev. Mod. Phys. **61**, 385 (1989).
[3] S. Meiboom, J. P. Sethna, P. W. Anderson, and W. F. Brinkman, Phys. Rev. Lett. **46**, 1216 (1981).
[4] F. Castles, S. M. Morris, E. M. Terentjev, and H. J. Coles, Phys. Rev. Lett. **104**, 157801 (2010).
[5] G. P. Alexander and J. M. Yeomans, Phys. Rev. Lett. **99**, 067801 (2007).
[6] G. P. Alexander, J. M. Yeomans, and S. Zumer, Faraday Discuss. **144**, 159 (2010).
[7] H. Kikuchi, M. Yokota, Y. Hisakado, H. Yang, and T. Kajiyama, Nat. Mater. **1**, 64 (2001).
[8] Y. Hisakado, H. Kikuchi, T. Nagamura, and T. Kajiyama, Adv. Mater. **17**, 96 (2005).
[9] Y. Haseba, H. Kikuchi, T. Nagamura, and T. Kajiyama, Adv. Mater. **17**, 2311 (2005).
[10] T. Iwata, K. Suzuki, N. Amaya, H. Higuchi, H. Masunaga, S. Sasaki, and H. Kikuchi, Macromolecules **42**, 2002 (2009).
[11] S. Y. Lu and L. C. Chien, Opt. Lett. **35**, 562 (2010).
[12] M. S. P. Shaffter and A. H. Windle, Adv. Mater. **11**, 937 (1999).
[13] C. Velasco-Santos, A. L. Martínez-Hernández, F. Fisher, R. S. Rouff, and V. M. Castano, J. Phys. D: Appl. Phys. **36**, 1423 (2003).
[14] T. Zhang, J. Ge, Y. Hu, and Y. Yin, Nano Lett. **7**, 3203 (2007).
[15] S. S. Banerjee and D. H. Chen, Chem. Mater. **19**, 6345 (2007).
[16] M. Suda, N. Kameyama, M. Suzuki, N. Kawamura, and Y. Einaga, Angew. Chem. Int. Ed. **47**, 160 (2007).
[17] D. Rangappa, T. Naka, A. Kondo, M. Ishii, T. Kobayashi, and T. Adschiri, J. Am. Chem. Soc. **129**, 11061 (2007).
[18] M. Taguchi, S. Takami, T. Adschiri, T. Nakane, K. Sato, and T. Naka, CrystEngComm **13**, 2841 (2011).
[19] P. R. Gerber, Mol. Cryst. Liq. Cryst. **116**, 197 (1985).
[20] K. Liang, G. Li, H. Toghiani, J. H. Koo, and C. U. Pittman, Jr., Chem. Mater. **18**, 301 (2006).
[21] D. Gnanasekaran, K. Madhavan, and B. S. R. Reddy, J. Sci. Ind. Res. **68**, 437 (2009).
[22] S.-W. Kuo and F.-C. Chang, Prog. Polym. Sci. **36**, 1649 (2011).
[23] H. Yoshida, Y. Tanaka, K. Kawamoto, H. Kubo, T. Tsuda, A. Fujii, S. Kuwabata, H. Kikuchi, and M. Ozaki, Appl. Phys. Exp. **2**, 121501 (2009).
[24] Y. Shiraishi, N. Toshima, K. Maeda, H. Yoshikawa, J. Xu, and S. Kobayashi, Appl. Phys. Lett. **81**, 2845 (2002).

[25] S.-T. Hur, M.-J. Gim, H. J. Yoo, S.-W. Choi, and H. Takezoe, Soft Matter **7**, 8800 (2011).

[26] See Supplemental Material at http://link.aps.org/supplemental/10.1103/PhysRevE.89.042502 for details of the blue phase temperature range dependence on the value of K_{33}/K_{11} ratios.

[27] L. Rao, Z. Ge, S.-T. Wu, and S. H. Lee, Phys. Lett. **95**, 231101 (2009).

[28] J. Yan, H.-C. Cheng, S. Gauza, Y. Li, M. Jiao, L. Rao, and S. T. Wu, Appl. Phys. Lett. **96**, 071105 (2010).

[29] M. Kim, B. G. Kang, M. S. Kim, M.-K. Kim, M.-H. Lee, S.-W. Kang, and H. L. Lee, Curr. Appl. Phys. **10**, e113 (2010).